Open Access Full Text Article

ORIGINAL RESEARCH

# Phytosynthesis of silver nanoparticles using *Artemisia marschalliana* Sprengel aerial part extract and assessment of their antioxidant, anticancer, and antibacterial properties

Soheil Salehi[1]
Seyed Ataollah Sadat Shandiz[2]
Farinaz Ghanbar[3]
Mohammad Raouf Darvish[4]
Mehdi Shafiee Ardestani[5]
Amir Mirzaie[2]
Mohsen Jafari[6]

[1]Department of Phytochemistry and Essential Oils Technology, Faculty of Pharmaceutical Chemistry, Pharmaceutical Sciences Branch, Islamic Azad University, Tehran (IAUPS), [2]Young Researchers and Elite Club, East Tehran Branch, Islamic Azad University, Tehran, [3]Department of Biology, Tehran North Branch, [4]Department of Chemistry, Shahre-Rey Branch, Islamic Azad University, Tehran, [5]Department of Radiopharmacy, Faculty of Pharmacy, Tehran University of Medical Sciences, Tehran, [6]Department of Biology, Faculty of Science, Shahid Chamran University of Ahvaz, Ahvaz, Iran

Correspondence: Seyed Ataollah Sadat Shandiz
Young Researchers and Elite Club, East Tehran Branch, Islamic Azad University, Shahid Bahonar St, Ghiamdasht, Khavaran Highway, Tehran, Iran
Tel/fax +98 21 3359 4337
Email atashandiz@yahoo.com

Mehdi Shafiee Ardestani
Department of Radiopharmacy, Faculty of Pharmacy, Tehran University of Medical Sciences, 16th Azar St, Enghelab Sq, Tehran, Iran
Tel/fax +98 21 6695 9098
Email shafieeardestani@tums.ac.ir

**Abstract:** A rapid phytosynthesis of silver nanoparticles (AgNPs) using an extract from the aerial parts of *Artemisia marschalliana* Sprengel was investigated in this study. The synthesized AgNPs using *A. marschalliana* extract was analyzed by UV–visible spectroscopy, X-ray diffraction, and Fourier transform infrared spectroscopy and further characterized by transmission electron microscopy, scanning electron microscopy, zeta potential, and energy-dispersive spectroscopy. Characteristic absorption bands of AgNPs were found near 430 nm in the UV–vis spectrum. Energy-dispersive spectroscopy analysis of AgNPs in the energy range 2–4 keV confirmed the silver signal due to surface plasmon resonance. Scanning electron microscopy and transmission electron microscopy results revealed that the AgNPs were mostly spherical with an average size ranging from 5 nm to 50 nm. The zeta potential value of −31 mV confirmed the stability of the AgNPs. AgNPs produced using the aqueous *A. marschalliana* extract might serve as a potent in vitro antioxidant, as revealed by 2,2-diphenyl-1-picryl hydrazyl assay. The present study demonstrates the anticancer properties of phytosynthesized AgNPs against human gastric carcinoma AGS cells. AgNPs exerted a dose-dependent inhibitory effect on the viability of cells. Real-time polymerase chain reaction was used for the investigation of *Bax* and *Bcl-2* gene expression in cancer and normal cell lines. Our findings show that the mRNA levels of pro-apoptotic *Bax* gene expression were significantly upregulated, while the expression of anti-apoptotic *Bcl-2* was declined in cells treated with AgNPs compared to normal cells. In addition, flow cytometric analysis showed that the number of early and late apoptotic AGS cells was significantly enhanced following treatment with AgNPs as compared to untreated cells. In addition, the AgNPs showed strong antibacterial properties against tested pathogenic bacteria such as *Staphylococcus aureus*, *Bacillus cereus*, *Acinetobacter baumannii*, and *Pseudomonas aeruginosa*. Based on the obtained data, we suggest that phytosynthesized AgNPs are good alternatives in the treatment of diseases because of the presence of bioactive agents.

**Keywords:** silver nanoparticles, *Artemisia marschalliana* Sprengel, anticancer, antibacterial

## Introduction

In recent years, the development of a novel protocol for the synthesis of metallic nanoparticles (NPs) with appropriate morphologies and sizes has been attracting the attention of researchers in the field of nanotechnology and biotechnology.[1,2] Nanomaterials research is an emerging field in the area of medicine, and the biosynthesis of NPs for many applications is an area of current interest.[3] Among these, silver nanoparticles (AgNPs) are attractive due to their potential applications in different fields, especially

in biosensors, pharmaceuticals, photonics, catalysis, and biomedicine, with potential for utilization as anti-angiogenic,[4] antimicrobial,[5] and anticancer[6] agents. AgNPs show strong toxicity to a wide range of microorganisms via oxidative stress, destructive effect on DNA, mitochondrial damage, and induction of apoptosis.[7,8] Generally, different physical and chemical methods are employed for the synthesis of AgNPs,[9] such as chemical reduction,[10] photochemical reduction,[11] electro-irradiation,[12] ultraviolet (UV) irradiation,[13] microware irradiation,[14] and laser-mediated synthesis.[15] Due to the presence of some toxic chemicals adsorbed on the surface of NPs, chemical strategies of their synthesis may have adverse impacts in their applications. In comparison with other methods, an eco-friendly, biological-mediated synthesis is the most preferred way for the synthesis of AgNPs, as it offers a one-step, solvent-free method that does not require reducing and stabilizing agents and provides a safe alternative to chemical methods and physical procedures.[16] Green synthesis of AgNPs using extracts of plants as capping and reducing agents has been beneficial to microorganisms due to their less biohazard.[17] Thus, considerable attention is being given to investigate the in vitro cytotoxicity of NPs using plant-based products. In addition, the rate of reduction of metal ions using plant extracts has been found to be much faster compared to microorganisms, and the stable formation of metallic NPs has been studied.[18] Several reports are available in the literature on the green synthesis of AgNPs using various plant extracts, including those from *Plumbago zeylanica*,[19] *Albizia adianthifolia*,[20] *Pulicaria glutinosa*,[21] *Eucalyptus leucoxylon*,[22] *Acacia leucophloea*,[23] *Chrysanthemum indicum* L.,[24] *Achillea biebersteinii*,[25] and *Lantana camara*.[26] Therefore, many plant-based products have been used in the synthesis of AgNPs. A few studies have been reported on *Artemisia* species extract as bioreductants for the preparation of AgNPs. Vijayakumar et al[27] have described a green synthesis of AgNPs using an aqueous leaf extract of *Artemisia nilagirica* as a stabilizing and reducing agent and investigated their antibacterial properties. Basavegowda et al[28] have reported the antibacterial and tyrosinase-inhibitory activities of Ag and Au NPs prepared from *Artemisia annua* leaf extract. In the present study, we devised a rapid and simple phytosynthesis of AgNPs using the aqueous extract from the aerial parts of *Artemisia marschalliana* Sprengel, which has not been reported so far. The protocol developed is simple, cost-effective, and viable. In addition, the reaction rate was extremely high and the reaction was completed in only 5 minutes. The genus *Artemisia*, belonging to the Asteraceae family, has long been used in folk medicine for the treatment of various ailments and diseases.[29] There are

~1,000 genera and >20,000 *Artemisia* species in the world. Many species of *Artemisia* have been used for some treatment purposes, including invigorating blood, relieving cough, and stopping pain, and as diuretic, anthelminthic, antiallergent, and antitoxic agents.[29] *Artemisia* is commonly found abundantly in Europe, Asia, and North America. Among the Asian *Artemisia* flora, 150 species were reported from the People's Republic of China, 50 species were recorded in Japan, and 34 species were found in Iran. *A. marschalliana* is a traditional Iranian medicinal plant and grows in Northwest Iran.[30] Further, the different organic compounds present in *A. marschalliana* plant extract (which were recognized via chromatography-mass-spectroscopy analysis of extract; data to be published elsewhere) include a large number of essential oils, hydroxycinnamic acids, and flavonoids, which are known for bioreduction of Ag+ ions. However, to our knowledge, this is the first study to investigate a rapid and simple approach for the synthesis of AgNPs using the extract of the aerial parts of *A. marschalliana* Sprengel as a reducing and stabilizing agent and to evaluate their biomedical properties. The prepared AgNPs were characterized by different physical techniques and evaluated for antiradical scavenging activity. The anti-proliferative properties of AgNPs were evaluated in human gastric carcinoma (AGS) and normal HEK293 cell lines. Moreover, the ability of the phytosynthesized AgNPs to induce apoptotic cell death was analyzed by quantitative real-time PCR and annexin V/propidium iodide (PI) staining. Further, its efficacy in inhibiting various pathogenic bacteria is also reported.

## Materials and methods
### Plant material and preparation of the extract
*A. marschalliana* Sprengel is cultivated in Tabriz, East Azarbaijan province, Iran. The plant was identified by Y. Ajani at the Herbarium of Iranian Biological Resources Center, Tehran, Iran (Voucher specimens No IBRCP1000141). Fresh aerial parts of *A. marschalliana* were washed thoroughly several times with distilled water and air-dried in the shade for 1–2 weeks. A total of 10 g of dried leaf powder was stirred in 1:1 ratio of 50 mL deionized water and 50 mL ethanol and then boiled for 20 minutes. The crude extract was filtered using Whatman No 1 filter paper (Whatman plc, Kent, UK). The remaining extract was kept in a refrigerator at 4°C until further use.

### Synthesis of AgNPs
For the synthesis of AgNPs, 100 mL of 0.01 mM aqueous solution of silver nitrate (EMD Millipore, Billerica, MA,

USA) was mixed with 4 mL of the aqueous plant extract, and the mixture was continuously stirred for 5 minutes at room temperature. The mixture was kept undisturbed until the colorless solution turned dark brown, revealing the reduction process of $Ag^+$ to $Ag^0$ NPs. The particles were then separated out by centrifugation at 12,000 rpm for 20 minutes. Then, the AgNPs were dried at 40°C for 2 hours prior to characterization.

## Characterization of AgNPs
### UV–visible spectroscopic characterization of AgNPs
The formation of AgNPs was monitored by a UV–visible spectrophotometer (UV 1601, Shimadzu), in the wavelength range of 250–850 nm.

### X-Ray diffraction analysis
Crystallographic structures of the bio-reduced AgNPs were examined by X-ray diffraction (XRD). The spectra were recorded in the scanning mode on a Burker AXS D8 X-ray diffractometer employing Cu Kα radiation, in range of $2\theta = 10°–80°$.

### Fourier transform infrared spectroscopic studies
Fourier transform infrared (FT-IR) spectroscopy studies were performed using a spectrum RX 1 instrument. The obtained samples were mixed with KBr, made into pellets, and analyzed to check the presence of functional groups in the phytoconstituents on the extract of *A. marschalliana* and the synthesized AgNPs. FT-IR spectra were scanned between 4,000 $cm^{-1}$ and 400 $cm^{-1}$ at a resolution of 4 $cm^{-1}$ in the transmittance mode.

### Field-emission scanning electron microscopy and energy-dispersive X-ray spectroscopy
Morphological studies of the prepared AgNPs were carried out by a field-emission scanning electron microscope (FE-SEM) (SIGMA; Carl Zeiss Meditec AG, Jena, Germany) using a gold film for loading the dried NPs in the instrument. Furthermore, the elemental composition of AgNPs was examined by an energy-dispersive spectroscopy analysis (EDS) analysis system.

### Transmission electron microscopy and zeta potentiometry
Examination of nanoparticle size and surface morphologies was performed by using a transmission electron microscope (TEM; JEOL model 1200EX) operating at 120 kV. Samples were prepared by placing a drop of AgNP–water dispersion on a carbon-coated copper grid and drying at room temperature.

A Malvern Zetasizer (Nano ZS90, UK) instrument was used to analyze the net surface charge of the NPs.

### 2,2-Diphenyl-1-picryl hydrazyl radical scavenging assay
The free-radical scavenging activity of AgNPs was quantitatively studied using 2,2-diphenyl-1-picryl hydrazyl (DPPH) assay. Briefly, different concentrations (50–450 μg/mL) of AgNPs and ascorbic acid (positive control) were taken separately and mixed with 3 mL of a methanolic solution of DPPH (final concentration 0.1 mM). The reaction mixture was shaken and kept for ~30 minutes at room temperature in the dark. Thereafter, the reduction of the DPPH radical was calculated by using a UV–visible spectrophotometer (UV 1601; Shimadzu Corporation, Kyoto, Japan) at 517 nm. The methanolic solution of DPPH without the sample served as a control. The percentage inhibition was measured according to the following equation:

$$\text{Percentage inhibition (\%)} = \frac{\text{Absorbance of control} - \text{Absorbance of test}}{\text{Absorbance of control}} \times 100 \quad (1)$$

## In vitro anticancer activity
### Cell lines and culture medium
The human gastric carcinoma (AGS) and human embryonic kidney (HEK293) cell lines were purchased from the Pasteur Institute cell bank, Tehran, Iran. The cells were grown adherently and maintained in Dulbecco's Modified Eagle's Medium supplemented with 10% fetal bovine serum, 2 mM glutamine, 1% antibiotic solution (100 U/mL of penicillin, 100 μg/mL of streptomycin), and 1 mM sodium pyruvate (all from Thermo Fisher Scientific, Waltham, MA, USA) in a 5% carbon dioxide ($CO_2$) cell incubator at 37°C. This study was approved by ethical committee of Islamic Azad University research council and was carried out based on the principles outlined in the Declaration of Helsinki.

### Cell viability assay
Cell viability was assessed by the 3-(4,5-dimethylthiazol-2-yl)-2,5-diphenyl-tetrazolium bromide (MTT) assay. In brief, the cells were counted and then distributed into 96-well plates at a density of 10,000 cells per well and incubated in a $CO_2$ incubator at 37°C for 24 hours. The AGS cancer cells were treated with a series of 3.125–100 μg/mL of phytosynthesized AgNPs in the 96-well plate. The stock concentration (5 mg/mL in phosphate buffered saline) of MTT was prepared, and 20 μL of MTT solution was added to each AgNP-treated well, followed by incubation at 37°C

and 5% $CO_2$ for 4 hours. Subsequently, the resulting purple formazan crystals were dissolved in dimethyl sulfoxide and then the optical density (OD) of each well was measured.[31] The absorbance at 570 nm was evaluated using a microplate reader (Bio-Rad 680; Microplate Master, Hercules, CA, USA). The effect of NPs on the cells was expressed as the percentage of cell viability compared to control, which was calculated according to the following formula: percentage of cell viability (%) = mean OD/control OD ×100.

## Analysis of apoptosis-related gene expression

A SYBR Green real-time quantitative PCR was carried out to quantify the expression levels of *Bax* and *Bcl-2* mRNAs in AGS and HEK293 cells. The cell lines were seeded into six-well plates ($5 \times 10^4$ cells/well) and incubated for 24 hours, and then the cells were treated with AgNPs for another 24 hours. Total cellular RNA was extracted from cells using the RNA-isolation kit (Qiagen, RNeasy Plus Mini Kit 50) according to the manufacturer's instructions. High-quality RNA was isolated for cDNA synthesis by using the PrimeScript™ first-strand cDNA synthesis kit (Takara, Japan) according to the manufacturer's protocol. The primers used for real-time PCR were as follows:

Forward 5′-TTGCTTCAGGGTTTCATCCAG-3′ and reverse 5′-AGCTTCTTGGTGGACGCATC-3′ for *Bax*, and forward 5′-TGTGGATGACTGAGTACCTGAACC-3′ and reverse 5′-CAGCCAGGAGAAATCAAACAGAG-3′ for *Bcl-2*. Also, the sequence of the forward primer for the house-keeping gene glyceraldehyde-3-phosphate dehydrogenase (*GAPDH*) was 5′-CGTCTGCCCTATCAACTTTCG-3′ and that of reverse primer was 5′-CGTTTCTCAGGCTCCCTCT-3′. The expression of the target gene was studied by using an ABI 7300 real-time PCR system (Thermo Fisher Scientific). Each PCR amplification reaction was performed in 20 µL reaction mixture containing 10 µL Power SYBR Green PCR Master Mix (2×), 1 µL of each primer (0.4 µM), 2 µL cDNA (100 ng), and 6 µL double-distilled water. After denaturation at 95°C for 10 minutes, 40 cycles were followed by 95°C for 15 seconds and 60°C for 1 minute in PCR cycling condition. Amplification stage was followed by a melting stage: at 95°C for 20 seconds, 60°C for 60 seconds, and 95°C for 20 seconds. The gene expression was determined using comparative threshold cycle (Ct). Afterward, the mean threshold cycle value of *GAPDH* as a reference gene was subtracted from the mean threshold cycle value of the target genes (*Bax*, *Bcl-2*) to obtain ΔCt, and ΔΔCt values of each sample were calculated from the corresponding Ct values. Finally, target/internal control gene expression ratio was calculated using the formula (ratio $=2^{-\Delta\Delta Ct}$).[32]

## In vitro apoptosis/necrosis assay

To determine apoptosis, a fluorescein isothiocyanate-annexin V and PI apoptosis detection kit (Hoffman-La Roche Ltd., Basel, Switzerland) was used according to the manufacturer's instruction. The AGS cell line ($1 \times 10^5$ cells/well) was incubated with AgNPs in a 24-well microplate for 24 hours, with untreated AGS cells as a positive control. Each experiment was carried out in duplicate.

## Determination of antibacterial property
### Bacterial strains

Four bacterial strains, namely *Staphylococcus aureus* (ATCC 6538), *Bacillus cereus* (ATCC 14579), *Acinetobacter baumannii* (ATCC 19606), and *Pseudomonas aeruginosa* (ATCC 15442), were obtained from the Iranian Research Organization for Science and Technology, Persian type culture collection, and were used for the determination of antibacterial effect of the synthesized AgNPs.

### Assessment of antibacterial activity of synthesized AgNPs

The disk diffusion method was used for the determination of antibacterial activity of the synthesized AgNPs. Briefly, the Muller Hinton agar (EMD Millipore) plates were inoculated with 1 mL ($1.0 \times 10^7$ colony-forming units) of bacterial cultures using spread-plating. After drying the plates, filter paper disks were put on the surface of plates and 50 µL of the synthesized AgNPs (0 ppm, 25 ppm, 50 ppm, 75 ppm, and 100 ppm) was introduced on all disks. Finally, the disks were placed on the plates and incubated for 24 hours at 37°C. The zone of inhibition was calculated by using a vernier caliper in triplicate. In all tests, standard ampicillin antibiotic disks and deionized water were used as positive and negative control, respectively.

### Statistical analysis

The values were expressed as the mean ± standard error of the mean, and all measurements were made in triplicate. The collected data were statistically analyzed using one-way analysis of variance with the SPSS/18 software. A $P$-value $<0.05$ was considered statistically significant.

## Results and discussion
### Phytosynthesis of AgNPs and UV–visible spectroscopic

This investigation focused on the preparation of AgNPs using an environmentally friendly, plant-mediated synthetic method. Several studies have demonstrated the green synthesis of metal NPs using aqueous extracts of plants for different

applications.[15,16] We successfully synthesized AgNPs using the aqueous extract of *A. marschalliana* Sprengel, which acted as a reducing agent. *A. marschalliana* is cheap and easily available, and there is no need to buy capping and reducing agents. Extracts from the aerial parts of *A. marschalliana* have not been used for the phytosynthesis of AgNPs so far. The reduction of silver ions into AgNPs was confirmed by the change in color of the silver nitrate solution to dark brown. This indicates that silver ions in the reaction medium have been converted to elemental silver. In most previous research investigations on the green synthesis of AgNPs, the rate of reaction was low, and it took several hours to complete. Basavegowda et al[28] showed the synthesis of Ag and Au NPs using the extracts from the leaves of *A. annua* within 10 minutes at room temperature. In our study, the rate of synthesis was very high, and it was completed in only 5 minutes. In this reaction, we can assume that the high amount of phenolic acids and flavonoids present in the extract of *A. marschalliana* might be playing a role of capping and reducing agents.[30] A majority of different compounds are known to play the role of capping and stabilizing agents in the bioreduction of silver salts. The absorption of the NPs is observed near 430 nm in the UV–vis spectrum, which is due to surface plasmon resonance of AgNPs (Figure 1). No additional peaks were seen in the spectrum, showing that the biosynthesized products are silver only.

## XRD analysis

The crystalline nature of the AgNPs produced by the plant extract was further confirmed by XRD analysis. Figure 2 shows a representative XRD pattern of the synthesized AgNPs using *A. marschalliana* extract. The four main characteristic peaks at 2θ values 38°, 46°, 64°, and 77° correspond to (111), (200), (220), and (311) planes of face-centered cubic (fcc) silver crystal, respectively. The XRD results are
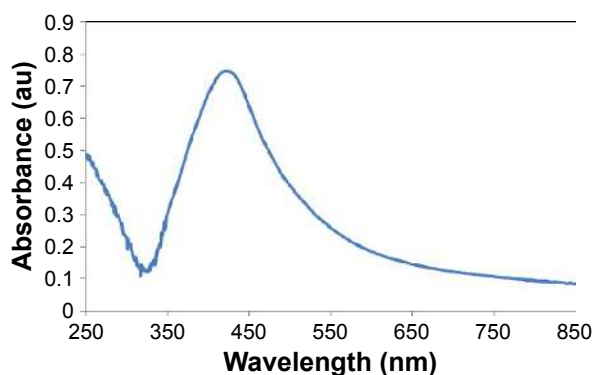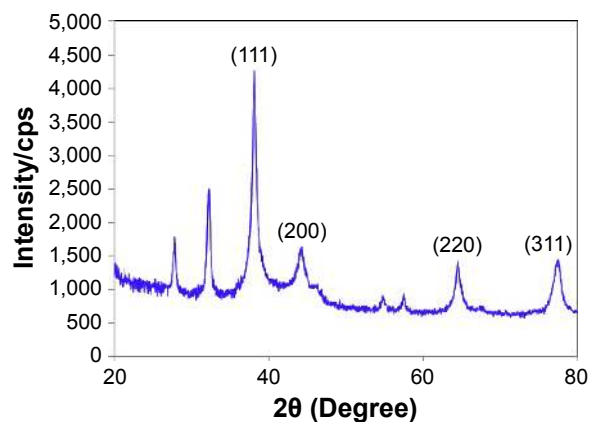
**Figure 2** XRD patterns of the synthesized AgNPs from *Artemisia marschalliana* aerial part extract.
**Abbreviations:** XRD, X-ray diffraction; AgNPs, silver nanoparticles; cps, counts per second.

in agreement with various reported values, confirming the cubic structure of phytosynthesized AgNPs.[24–27]

## FT-IR analysis of AgNPs

FT-IR measurements were carried out to identify the potential biomolecules in *A. marschalliana* extract responsible for the reduction of the synthesized NPs. Figure 3A and B shows the FT-IR spectra of the extract prepared from powdered aerial parts of *A. marschalliana* and AgNPs, respectively. The strong band at 3,463 cm$^{-1}$ in *A. marschalliana* powder was attributed to the O–H stretching band of alcohols and phenols,[33] which shifted to 3,510 cm$^{-1}$ in AgNPs apparently because of protein binding. Absorption peaks located at 2,962 and 2,823 cm$^{-1}$ corresponded to alkane C–H stretching vibrational modes.[34] A more intense peak was observed at 1,624 cm$^{-1}$, signifying the presence of carbonyl (C–O) stretching vibrations.[35] The medium-intensity peak at 1,398 cm$^{-1}$, which is absent from the AgNPs FT-IR spectrum, was assigned to the C–N stretching vibrations of aromatic
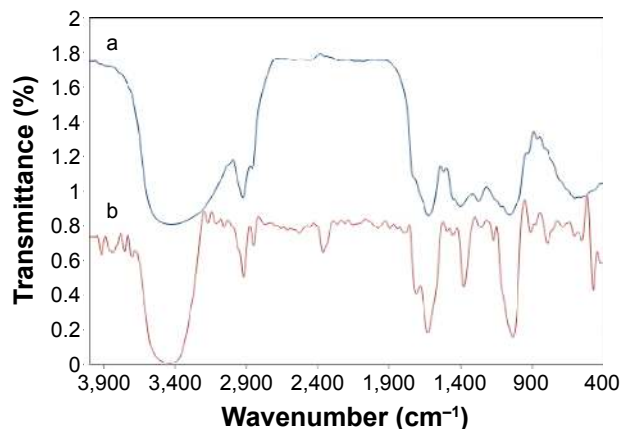
**Figure 1** UV–vis absorption spectrum of the phytosynthesized AgNPs.
**Abbreviations:** UV–vis, ultraviolet–visible; AgNPs, silver nanoparticles.

**Figure 3** FT-IR spectra of (a) *Artemisia marschalliana* Sprengel aerial part extract and (b) AgNPs.
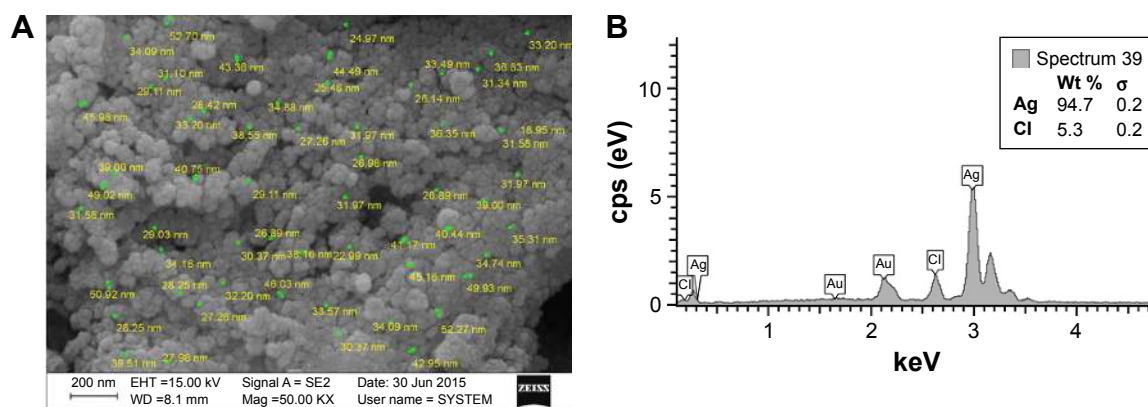**Abbreviations:** FT-IR, Fourier transform infrared; AgNPs, silver nanoparticles.

**Figure 4** Morphological study and elemental composition of prepared AgNPs.
**Notes:** (**A**) FE-SEM images of synthesized AgNPs using aerial part extract of *Artemisia marschalliana* Sprengel. (**B**) EDS spectrum of the prepared AgNPs. A strong peak at 3 keV confirms the existence of Ag.
**Abbreviations:** FE-SEM, field-emission scanning electron microscopy; AgNPs, silver nanoparticles; EDS, energy-dispersive spectroscopy analysis; cps, counts per second; EHT, extra high tension; WD, working distance; Mag, magnification.

amines, and the band at 1,049 cm$^{-1}$, which is characteristic of glycoside or ether (C–O–C) groups, shifted to 1,038 cm$^{-1}$ in AgNPs.

Based on the earlier observations, we may conclude that functional groups such as hydroxyl, amide, and carbonyl present in the *A. marschalliana* extract might be responsible for the bioreduction of Ag$^+$ to AgNPs.

## FE-SEM and EDS

The FE-SEM images of the synthesized AgNPs showed the particles to be spherical in shape. The average size of particles was 5–50 nm (Figure 4A). The elemental composition of the silver particles was studied by EDS analysis (Figure 4B), which revealed strong signals in silver region. Usually, metallic AgNPs show a typical absorption peak at ~3 keV due to surface plasmon resonance.[14,21] EDS analysis revealed the presence of silver (94.7%) without any contamination. The appearance of other signals in the image, such as chlorine,

confirmed the presence of organic moieties (from the plant extract), which correspond to the biomolecules capping over the phytosynthesized AgNPs.

## TEM and zeta potentiometry

A typical TEM micrograph of AgNPs is shown in Figure 5A. It is apparent from the figure that the obtained Ag particles are in the nanometer range with spherical shapes and the size of the particle varied from 5 nm to 20 nm. The particle size histogram of the synthesized AgNPs (Figure 5B) shows that the particles have an average size of 7.94 nm. The surface charges of the NPs were determined by the zeta potential value. A negative zeta potential of approximately −31 mV was recorded in the current study, suggesting higher stability of the synthesized AgNPs (Figure 6). The greater negative surface charge potential value may be attributed to the effective functional constituents as capping agents present in the ethanol extract of *A. marschalliana* Sprengel.
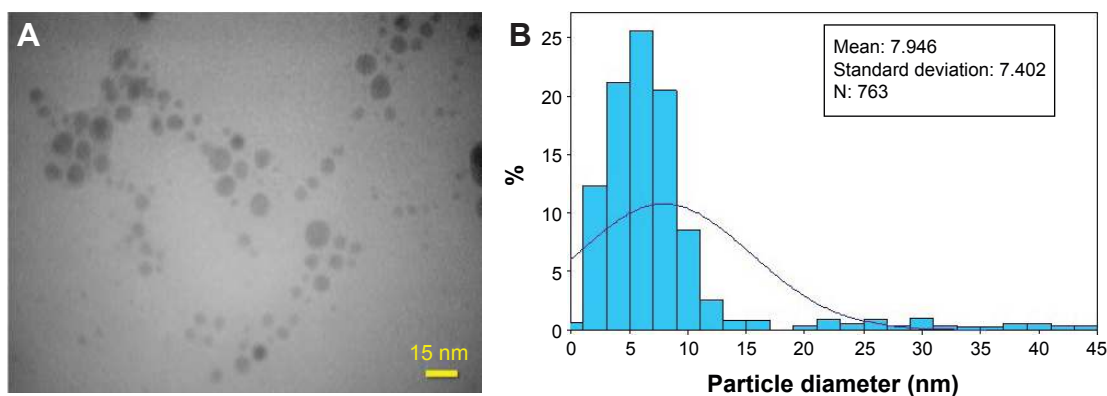


**Figure 5** Transmission electron microscopy image and corresponding histogram showing particle size distribution of prepared AgNPs.
**Notes:** (**A**) TEM image and (**B**) particles size distribution of AgNPs synthesized by *A. marschalliana* extract.
**Abbreviations:** TEM, transmission electron microscopy; AgNPs, silver nanoparticles; *A. marschalliana*, *Artemisia marschalliana*.
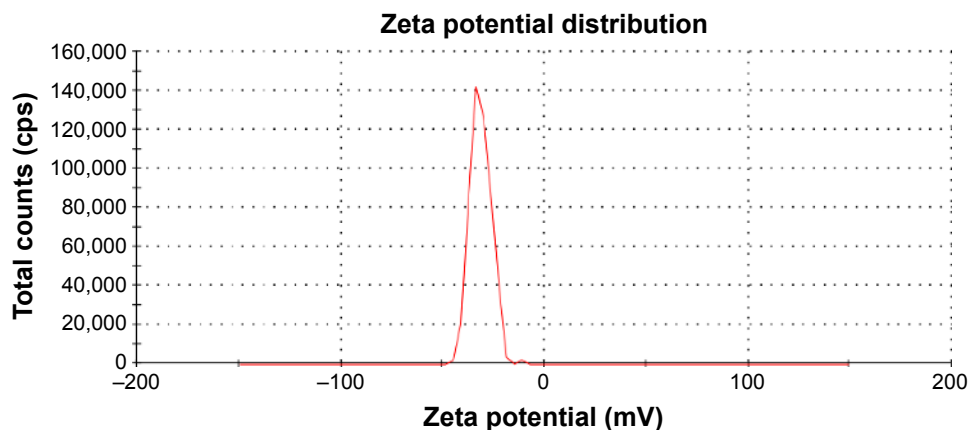
**Figure 6** Zeta potential measurement of the phytosynthesized AgNPs.
**Abbreviations:** AgNPs, silver nanoparticles; cps, counts per second.

## DPPH free-radical scavenging assay

The effect of various concentrations of AgNPs on DPPH radical scavenging activity is shown in Figure 7. DPPH is a stable free radical compound and receives electrons or hydrogen from the AgNPs. The free-radical scavenging results show that the percentage of inhibition increases with increasing concentration of AgNPs. The results of our study thus confirmed the radical scavenging activity of AgNPs. The potential reason for the antioxidant activity of AgNPs may be correlated to the existence of bioactive compounds present in them. The highest percentage of inhibition monitored in AgNPs was 61%, which was lower than that of ascorbic acid at 450 µg/mL (92%). Similar studies with enhanced DPPH scavenging activity by AgNPs from leaf extracts[35] have been investigated, and enhanced DPPH scavenging properties by selenium-,

platinum-, torolex-, and chitosan-coated gold NPs[36–39] have also been reported.

## Cytotoxicity studies

The cell viability of AgNPs was analyzed by using MTT assay (Figure 8). Incubation of the AGS cells at different concentrations (3.125 µg/mL, 6.25 µg/mL, 12.5 µg/mL, 25 µg/mL, 50 µg/mL, and 100 µg/mL) of AgNPs after 24 hours showed a dose-dependent decrease in cell viability compared to control. Our results showed that the AGS cancer cell viability was clearly proportional to the concentration of the phytosynthesized AgNPs. The corresponding $IC_{50}$ value of AgNPs on gastric cancer AGS cell line was calculated to be 21.05 µg/mL. The cell viability decreased to 3.125 µg/mL and progressively declined according to the concentration. When the concentration of AgNPs reached
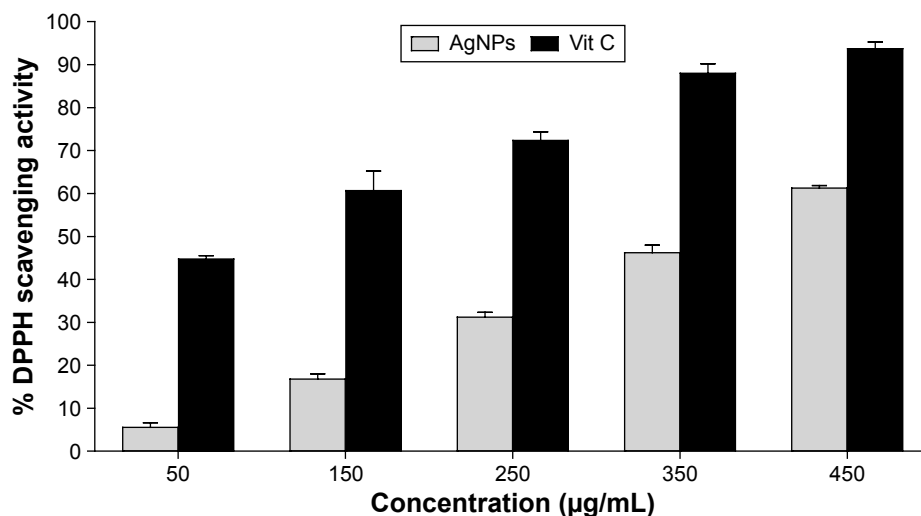


**Figure 7** DPPH radical scavenging activity of AgNPs synthesized by *Artemisia marschalliana* Sprengel extract.
**Abbreviations:** DPPH, 2,2-diphenyl-1-picryl hydrazyl; AgNPs, silver nanoparticles; Vit, vitamin.
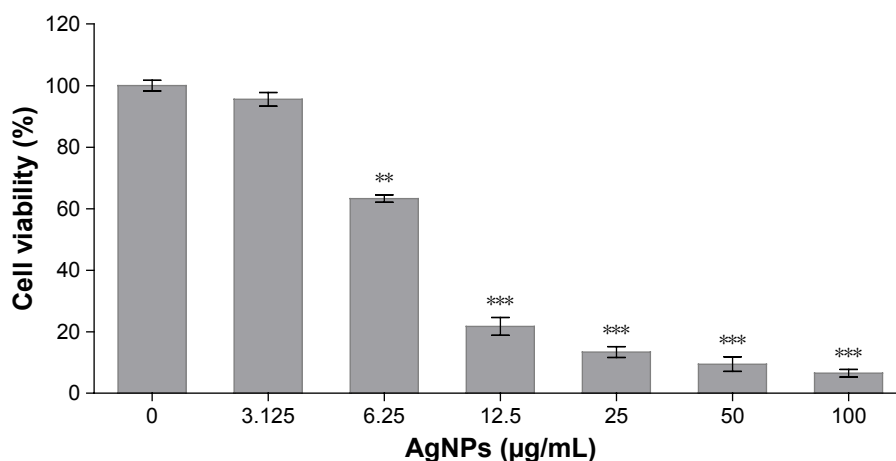
**Figure 8** MTT assay results confirming the in vitro cytotoxicity effect of the synthesized AgNPs against AGS cells after 24 hours.
**Notes:** Data are expressed as mean ± SD of three experiments. Percentage of viability is expressed relative to untreated controls (\*\*$P<0.01$; \*\*\*$P<0.001$).
**Abbreviations:** MTT, 3-(4,5-dimethylthiazol-2-yl)-2,5-diphenyl-tetrazolium bromide; AgNPs, silver nanoparticles; SD, standard deviation.

100 µg/mL, ~6.51% viable cells existed. This is the first work to report the cytotoxicity of AgNPs synthesized using aerial part extract of *A. marschalliana* Sprengel against human gastric carcinoma AGS cell line. Hackenberg et al[40] have observed that 10 µg/mL of AgNPs decreased human mesenchymal stem cell survival during 24 hours of exposure. Also, Vivek et al[41] demonstrated that the dose-dependent cytotoxicity effect of green synthesized AgNPs significantly increased with the concentration of NPs. Further investigations have been performed, which showed that AgNPs were taken up by mammalian cells through different mechanisms such as phagocytosis, pinocytosis, and endocytosis and interact with the cellular material.[41–44] From our results, it can be concluded that AgNPs could have induced the generation of reactive oxygen species, which damage DNA and/or the mitochondria-dependent (intrinsic) apoptosis pathway, leading to cell death.

## Analysis of apoptosis-related gene expression

The expression of pro-apoptotic and anti-apoptotic genes at the mRNA level in AgNP-exposed AGS and HEK293 cell lines was studied using quantitative real-time PCR (Figure 9). Our findings show that the mRNA level of *Bax* was significantly upregulated, while the expression of the anti-apoptotic *Bcl-2* was significantly diminished in cells treated with AgNPs compared to normal cells. Therefore, the *Bax/Bcl-2* ratio increased. *GAPDH* was used as an internal standard control gene for real-time PCR. These effects could be attributed to the increased sensitivity of AGS cell line to induce apoptosis when

exposed to AgNPs. Previous studies have shown that AgNPs have cytotoxic effects in different cell types and apoptosis-inducing properties.[20,25,41]

## In vitro apoptosis/necrosis assay

Further experiments were conducted with fluorescein isothiocyanate-annexin V and PI staining and flow cytometric analysis. During early apoptosis, phosphatidyl serins (PS) in the membrane translocate to the outer leaflet of the cell membrane. Annexin–V/PI detection assay can be used for detecting the exposed PS by flow cytometry. Annexin V stains PS of the early and late apoptotic cells, while PI detects the nucleus of the cells, which have a disrupted integrity due to necrosis.[45] Hence, the annexin V+/PI− cells detect early stage of apoptosis, and annexin V+/PI+ cells exhibit late stage of apoptosis or necrosis.[46] Based on the annexin V/PI staining results, many annexin V+/PI+ cells were detected in the AGS cells treated with 21.05 µM of AgNPs, showing the early and late stages of apoptosis. Figure 10 shows that
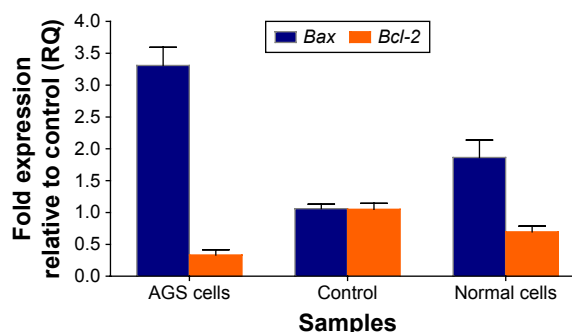


**Figure 9** Effect of AgNPs on *Bax* and *Bcl-2* expression in AGS and HEK293 cell lines.
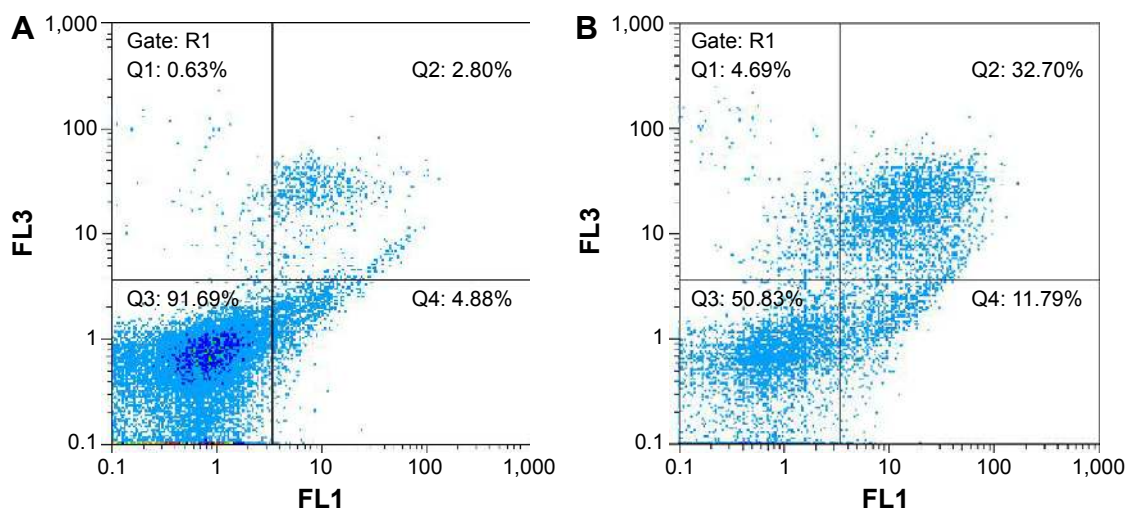**Abbreviations:** AgNPs, silver nanoparticles; RQ, relative quantitative.

**Figure 10** Flow cytometric analyses by annexin V-FLUOS (FL1) (*x*-axis) and PI (FL3) (*y*-axis) double staining of AGS cells treated with the phytosynthesized AgNPs at 24 hours.
**Notes:** The apoptotic cells stained by annexin V and unstained by propidium iodide in the lower right quadrant (LR), late apoptotic (annexin $V^+/PI^+$) populations were presented in the upper right quadrant (UR), and necrotic cell (annexin $V^-/PI^+$) populations were located in the upper left quadrant (UL). Dot plots of annexin V/PI staining are shown in (**A**) untreated AGS cells. (**B**) AGS cells treated with 21.05 µg/mL AgNPs exhibited 11.79% early-stage apoptosis and 32.70% late-stage apoptosis.
**Abbreviations:** PI, propidium iodide; AgNPs, silver nanoparticles; FLUOS, fluorescein.

there is ~7% and 30% increase in early and late apoptotic population in the treated AGS cells, respectively, compared to control AGS cells. These results show that the cytotoxicity of AgNPs toward AGS cells was chiefly due to their ability to induce apoptosis rather than necrosis.

## Antibacterial activity

Several recent studies have demonstrated that biosynthesized AgNPs have strong antimicrobial effects in different microorganisms.[47] The antibacterial activities of various concentrations of AgNPs were studied on *S. aureus*, *B. cereus*, *A. baumannii*, and *P. aeruginosa*. It is evident from our study that the phytosynthesized AgNPs showed inhibitory activity against pathogenic bacteria at different concentrations (Figure 11); the data are presented in Table 1. Among the different tested bacterial strains, *S. aureus and P. aeruginosa* were the most susceptible toward the AgNPs. The largest inhibition zone (15.5±1.32 mm) at 100 ppm concentration of AgNPs was measured with *S. aureus* and the least (3.11±1.58 mm) was at 25 ppm concentration with *B. cereus*. From our study, it is clear that phytosynthesized AgNPs can compete with antibiotics used for bacterial treatment. To date, no mechanism has been suggested to explain the inhibitory effect of nanosilver on microorganisms. However, several methodologies have been suggested to describe the inhibitory action of silver ions on bacteria. Sondi and Salopek-Sondi[48] reported that interruption

of bacterial membrane morphology shows a significant increase in AgNP permeability, resulting in uncontrolled transport through the cell membrane and eventually causing cell death. It is assumed that silver ions released from AgNPs can bind to oxygen, sulfur, and nitrogen of fundamental biomolecules, thereby inhibiting respiration and bacterial growth. Another hypothesized mechanism involves the effects of $Ag^+$ on the inactivation of DNA replication ability and cellular proteins necessary for adenosine triphosphate (ATP) synthesis in bacteria.[49]

## Conclusion

This is the first study to report a plant-mediated approach for the synthesis of AgNPs using the extract from the aerial parts of *A. marschalliana* as a reducing and capping agent without any toxic or harmful reducing agents or chemicals, such as sodium borohydrate, or any dispersing or capping agents. This method is simple, rapid, and eco-friendly for the synthesis of AgNPs. Due to the capping and reducing nature of the phytoconstituents in the *A. marschalliana* Sprengel extract, a cap was formed around the Ag ions of the AgNPs, making them stable. The structural and compositional characterization of the synthesized AgNPs were done by using UV–vis spectroscopy, TEM, FE-SEM, FT-IR, EDS, zeta potential, and XRD analysis, which proved the presence of AgNPs with an average size of 5–50 nm. From the results of DPPH radical scavenging assay, the AgNPs
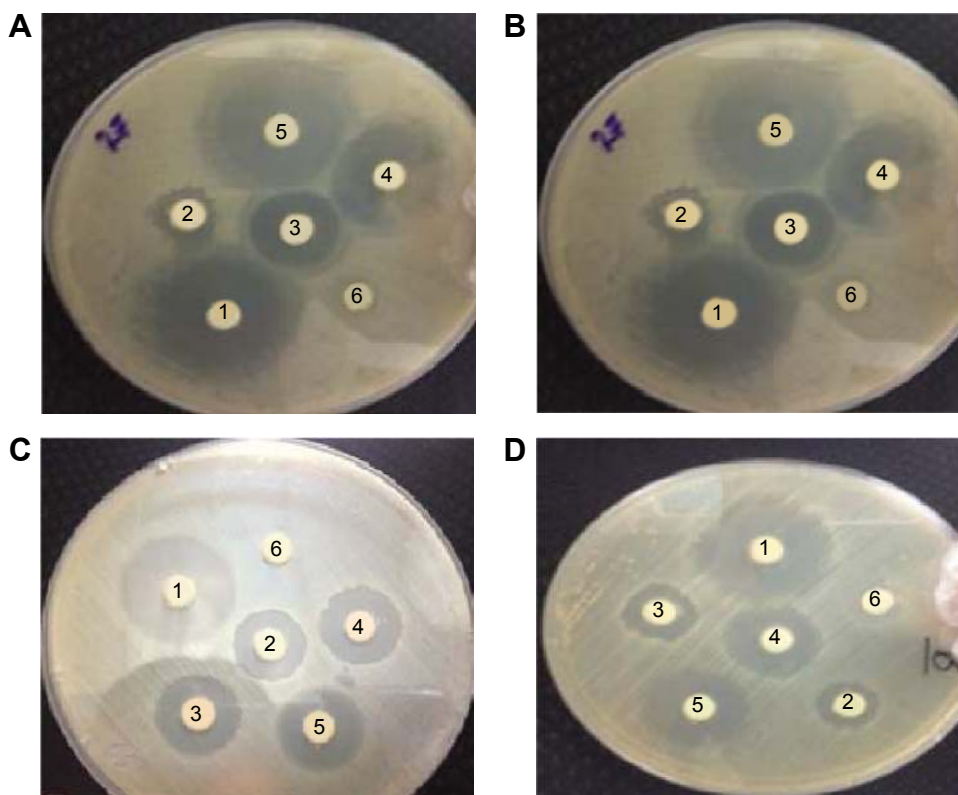
**Figure 11** Antibacterial activity of AgNPs against bacteria versus ampicillin.
**Notes:** (**A**) *S. aureus*. (**B**) *P. aeroginosa*. (**C**) *A. bumanii*. (**D**) *B. cereus*. The numbers on plates indicate the silver nanoparticle concentrations. 1, ampicillin; 2, 25 ppm; 3, 50 ppm; 4, 75 ppm; 5, 100 ppm; 6, 0 ppm (negative control).
**Abbreviations:** AgNPs, silver nanoparticles; *S. aureus, Staphylococcus aureus*; *P. aeruginosa, Pseudomonas aeruginosa*; *A. baumannii, Acinetobacter baumannii*; *B. cereus, Bacillus cereus*.

were shown to possess antioxidant property at different concentrations. Our study showed that the synthesized AgNPs exhibit anticancer effect on human gastric cancer AGS cell line. In addition, mRNA levels of the pro-apoptotic *Bax* gene expression were significantly upregulated, while the expression of the anti-apoptotic *Bcl-2* gene was significantly reduced in cells treated with AgNPs compared to normal cells. Annexin V/PI staining results showed that the cytotoxicity of AgNPs toward AGS cells was chiefly due to their ability to induce apoptosis rather than necrosis. In addition, the phytosynthesized AgNPs demonstrated promising antibacterial activity against both Gram-negative (*A. baumannii* and *P. aeruginosa*) and Gram-positive (*S. aureus, B. cereus*) bacteria. However, a stronger inhibition was seen in *S. aureus*, a Gram-negative bacterium, compared to Gram-positive bacteria. Based on the obtained data, we suggest that the phytosynthesized AgNPs are good alternatives in medicinal and therapeutic applications.

**Table 1** Antibacterial activity of the synthesized AgNPs on pathogenic bacteria and ampicillin as a positive control

| AgNPs conc (ppm) | Zone of inhibition against human pathogenic bacteria | | | |
|---|---|---|---|---|
| | *S. aureus* | *P. aeruginosa* | *A. baumannii* | *B. cereus* |
| 0 | 0 | 0 | 0 | 0 |
| 25 | 3.51±1.33 | 3.46±0.75 | 3.35±0.89 | 3.11±1.58 |
| 50 | 9.62±1.21 | 7.11±0.55 | 6.76±0.44 | 4.11±1.72 |
| 75 | 13.8±1.55 | 10.36±0.66 | 8.22±0.77 | 6.12±1.42 |
| 100 | 15.50±1.32 | 13.38±0.78 | 11.45±0.9 | 8.66±1.20 |
| Ampicillin | 18.77±1.23 | 17.22±0.98 | 15.0±0.60 | 12.3±1.15 |

**Note:** Each value represents the mean ± SE of three replicates.
**Abbreviations:** AgNPs, silver nanoparticles; conc, concentration; SE, standard error; *S. aureus, Staphylococcus aureus*; *P. aeruginosa, Pseudomonas aeruginosa*; *A. baumannii, Acinetobacter baumannii*; *B. cereus, Bacillus cereus*.

## Disclosure

The authors report no conflicts of interest in this work.

## References

1. Sharma VK, Yngard RA, Lin Y. Silver nanoparticles: green synthesis and their antimicrobial activities. *Adv Colloid Interface Sci*. 2009; 145(1–2):83–96.
2. Gopinath V, Mubarak AD, Priyadarshini S, Prishadharsshini NM, Thajuddin N, Velusamy P. Biosynthesis of silver nanoparticles from *Tribulus terrestris* and its antimicrobial activity: a novel biological approach. *Colloids Surf B Biointerfaces*. 2012;96:69–74.
3. Adams FC, Barbante C. Nanoscience, nanotechnology and spectrometry. *Spectrochim Acta Part B At Spectrosc*. 2013;86:3–13.
4. Gurunathan S, Lee KJ, Kalishwaralal K, Sheikpranbabu S, Vaidyanathan R, Eom SH. Antiangiogenic properties of silver nanoparticles. *Biomaterials*. 2009;30(31):6341–6350.
5. Oei JD, Zhao WW, Chu L, et al. Antimicrobial acrylic materials with in situ generated silver nanoparticles. *J Biomed Mater Res B Appl Biomater*. 2012;100(2):409–415.
6. Kalishwaralal K, Banumathi E, Pandian SRK, et al. Silver nanoparticles inhibit VEGF induced cell proliferation and migration in bovine retinal endothelial cells. *Colloids Surf B Biointerfaces*. 2009;73(1):51–57.
7. Chau CF, Wu SH, Yen GC. The development of regulations for food nanotechnology. *Trends Food Sci Technol*. 2007;18:269–280.
8. Panyala NR, Pena-Mendez EM, Havel J. Silver or silver nanoparticles: a hazardous threat to the environment and human health? *J Appl Biomed*. 2008;6:117–129.
9. Ezzatzadeh E, Farjam MH, Rustaiyan A. Comparative evaluation of antioxidant and antimicrobial activity of crude extract and secondary metabolites isolated from *Artemisia kulbadica*. *Asian Pac J Trop Dis*. 2012;2:431–434.
10. Tao A, Sinsermsuksaku P, Yang P. Polyhedral silver nanocrystals with distinct scattering signatures. *Angew Chem Int Ed*. 2006;45(28): 4597–4601.
11. Malice K, Witcombb MS, Scurrella MS. Self-assembly of silver nanoparticles in a polymer solvent: formation of a nanochain through nanoscale soldering. *Mater Chem Phys*. 2005;90:221–224.
12. Li K, Zhang FS. A novel approach for preparing silver nanoparticles under electron beam irradiation. *J Nanopart Res*. 2010;12(4):1423–1428.
13. Le AT, Tam LT, Tam PD, et al. Synthesis of oleic acid-stabilized silver nanoparticles and analysis of their antibacterial activity. *Mater Sci Eng C*. 2010;30(6):910–916.
14. Nadagouda MN, Speth TF, Varma RS. Microwave-assisted green synthesis of silver nanostructures. *Acc Chem Res*. 2011;44(7):469–478.
15. Zamiri R, Zakaria A, Abbastabar H, Darroudi M, Husin MS, Mahdi MA. Laser-fabricated cost or oil-capped silver nanoparticles. *Int J Nanomedicine*. 2011;6:565–568.
16. Hutchison JE. Greener nanoscience: a proactive approach to advancing applications and reducing implications of nanotechnology. *ACS Nano*. 2008;2:395–402.
17. Li H, Carter JD, LaBean TH. Nanofabrication by DNA self-assembly. *Mater Today*. 2009;12(5):24–32.
18. Zayed WH, Eisa WH, Shabaka AA. *Malva parviflora* extract assisted green synthesis of silver nanoparticles. *Spectrochim Acta A Mol Biomol Spectrosc*. 2012;98:423–428.
19. Salunke GR, Ghosh S, Kumar RJS, et al. Rapid efficient synthesis and characterization of silver, gold, and bimetallic nanoparticles from the medicinal plant *Plumbago zeylanica* and their application in biofilm control. *Int J Nanomedicine*. 2014;9:2635–2653.
20. Govender R, Phulukdaree A, Gengan RM, Anand K, Chuturgoon AA. Silver nanoparticles of *Albizia adianthifolia*: the induction of apoptosis in human lung carcinoma cell line. *J Nanobiotechnology*. 2013;11:5.
21. Khan M, Khan ST, Khan M, et al. Antibacterial properties of silver nanoparticles synthesized using *Pulicaria glutinosa* plant extract as a green bioreductant. *Int J Nanomedicine*. 2014;9:3551–3565.

22. Nasrabadi MR, Pourmortazavi SM, Sadat Shandiz SA, Ahmadi F, Batooli H. Green synthesis of silver nanoparticles using *Eucalyptus leucoxylon* leaves extract and evaluating the antioxidant activities of extract. *Nat Prod Res*. 2014;28(22):1964–1969.
23. Murugan K, Senthilkumar B, Senbagam D, Al-Sohaibani S. Biosynthesis of silver nanoparticles using *Acacia leucophloea* extract and their antibacterial activity. *Int J Nanomedicine*. 2014;9:2431–2438.
24. Rokiyaraj SA, Arasu MV, Vincent S, et al. Rapid green synthesis of silver nanoparticles from *Chrysanthemum indicum* L and its antibacterial and cytotoxic effects: an in vitro study. *Int J Nanomedicine*. 2014; 9:379–388.
25. Baharara J, Namvar F, Ramezani T, Mousavi M, Mohamad R. Silver nanoparticles biosynthesized using *Achillea biebersteinii* flower extract: apoptosis induction in MCF-7 cells via caspase activation and regulation of Bax and Bcl-2 gene expression. *Molecules*. 2015;20:2693–2706.
26. Ajitha B, Ashok KRY, Sreedhara RP. Green synthesis and characterization of silver nanoparticles using *Lantana camara* leaf extract. *Mater Sci Eng C*. 2015;49(1):373–381.
27. Vijayakumar M, Priya K, Nancy FT, Noorlidah A, Ahmed ABA. Biosynthesis, characterization and antibacterial effect of plant-mediated silver nanoparticles using *Artemisia nilagirica*. *Ind Crops Prod*. 2013; 41:235–240.
28. Basavegowda N, Idhayadhulla A, Lee YR. Preparation of Au and Ag nanoparticles using *Artemisia annua* and their *in vitro* antibacterial and tyrosinase inhibitory activities. *Mater Sci Eng C Mater Biol Appl*. 2014;43:58–64.
29. Romero MR, Serrano MA, Vallejo M, Efferth T, Alvarez M, Marin JJ. Antiviral effect of artemisinin from *Artemisia annua* against a model member of the Flaviviridae family, the bovine viral diarrhoea virus (BVDV). *Planta Med*. 2006;72(13):1169–1174.
30. Nahrevanian H, Milan BS, Kazemi M, Hajhosseini R, Mashhadi SS, Nahrevanian S. Antimalarial effects of Iranian flora *Artemisia sieberi* on *Plasmodium berghei in vivo* in mice and phytochemistry analysis of its herbal extracts. *Malar Res Treat*. 2012;2012:727032.
31. Sadat Shandiz SA, Khosravani M, Mohammadi S, et al. Evaluation of imatinib mesylate (Gleevec) on *KAI1/CD82* gene expression in breast cancer MCF-7 cells using quantitative real-time PCR. *Asian Pac J Trop Biomed*. 2016;6(2):159–163.
32. Sadat Shandiz SA, ShafieeArdestani M, Irani SH, Shahbazzadeh D. Imatinib induces down regulation of Bcl-2 an anti-apoptotic protein in prostate cancer PC-3 cell line. *Adv Stud Biol*. 2015;7:17–27.
33. Preeti D, Mausumi M. *In-vitro* free radical scavenging activity of biosynthesized gold and silver nanoparticles using *Prunus armeniaca* (apricot) fruit extract. *J Nanopart Res*. 2013;15:1366.
34. Noruzi M, Zare D, Davoodi D. A rapid biosynthesis route for the preparation of gold nanoparticles by aqueous extract of cypress leaves at room temperature. *Spectrochim Acta A*. 2012;94:84–88.
35. Saravanakumar A, Ganesh M, Jayaparakash J, Jang HT. Biosynthesis of silver nanoparticles using *Cassia tora* leaf extract and its antioxidant and antibacterial activities. *J Ind Eng Chem*. 2015;28:277–281.
36. Gao XY, Zhang J, Zhang L. Hollow sphere selenium nanoparticles: their in vitro anti hydroxyl radical effect. *Adv Mater*. 2002;14:290–293.
37. Saikia JP, Paul S, Konwar BK, Samdarshi SK. Nickel oxide nanoparticles: a novel antioxidant. *Colloids Surf B Biointerfaces*. 2010;78(1): 146–148.
38. Nie Z, Liu KJ, Zhong CJ, et al. Enhanced radical scavenging activity by antioxidant-functionalized gold nanoparticles: a novel inspiration for development of new artificial antioxidants. *Free Radic Biol Med*. 2007;43(9):1243–1254.
39. Raghunandan D, Bedre MD, Basavaraja S, Sawle B, Manjunath SY, Venkataraman A. Rapid biosynthesis of irregular shaped gold nanoparticles from macerated aqueous extracellular dried clove buds solution. *Colloids Surf B Biointerfaces*. 2010;79:235–240.
40. Hackenberg S, Scherzed A, Kessler M, et al. Silver nanoparticle: evaluation of DNA damage, toxicity and functional impairment in human mesenchymal stem cells. *Toxicol Lett*. 2011;201(1):27–33.

41. Vivek R, Thangam R, Muthuchelian K, Gunasekaran P, Kaveri K, Kannan S. Green biosynthesis of silver nanoparticles from *Annona squamosa* leaf extract and it's *in vitro* cytotoxic effect on MCF-7 cells. *Process Biochem*. 2012;47:2405–2410.

42. Tiwari DK, Jin T, Behari J. Dose-dependent in-vivo toxicity assessment of silver nanoparticle in Wistar rats. *Toxicol Mech Methods*. 2011; 21(1):13–24.

43. Sankar R, Karthik A, Prabu A, Karthik S, Shivashankari KS, Ravikumar V. *Origanum vulgare* mediated biosynthesis of silver nanoparticles for its antibacterial and anticancer activity. *Colloids Surf B Biointerfaces*. 2013;108:80–84.

44. Patel B, Shah VR, Bavadekar SA. Anti-proliferative effects of carvacrol on human prostate cancer cell line, LNCaP. *FASEB J*. 2012;26: 1037–1045.

45. Sadat Shandiz SA, Farasati S, Saeedi B, et al. Up regulation of *KAI1* gene expression and apoptosis effect of imatinib mesylate in gastric adenocarcinoma (AGS) cell line. *Asian Pac J Trop Dis*. 2016;6(2): 120–125.

46. Zhang G, Gurtu V, Kain SR, Yan G. Early detection of apoptosis using a fluorescent conjugate of annexin V. *Biotechniques*. 1997;23: 525–531.

47. Puiso J, EJonkuviene D, Macioniene I, Salomskiene J, Jasutiene I, Kondrotas R. Biosynthesis of silver nanoparticles using lingonberry and cranberry juices and their antimicrobial activity. *Colloids Surf B Biointerfaces*. 2014;121:214–221.

48. Sondi I, Salopek-Sondi B. Silver nanoparticles as antimicrobial agent: a case study on *E. coli* as a model for Gram-negative bacteria. *J Colloid Interface Sci*. 2004;275(1):177–182.

49. Feng QL, Wu J, Chen GQ, Cui FZ, Kim TN, Kim JO. Mechanistic study of the antibacterial effect of silver ions on *Escherichia coli* and *Staphylococcus aureus*. *J Biomed Mater Res*. 2000;52:662–668.